Investigating the aggregation of Alzheimer's disease-associated proteins in *S. cerevisiae*

A Dissertation
Presented to
The Academic Faculty

by

Julia Denniss

In Partial Fulfillment
of the Requirements for the Degree
B.S. in Biology with Research Option in the
School of Biological Sciences

Georgia Institute of Technology
May 2019

INVESTIGATING THE AGGREGATION OF ALZHEIMER'S DISEASE-ASSOCIATED PROTEINS IN *S. CEREVISIAE*

Approved by:

Dr. Yury Chernoff, Advisor
School of Biology
Georgia Institute of Technology

Dr. Michael Goodisman
School of Biology
Georgia Institute of Technology

Dr. Francesca Storici
School of Biology
Georgia Institute of Technology

Date Approved: [Date approved by committee]

ACKNOWLEDGEMENTS

I would like to thank my mentor, PhD candidate Zack Deckner, for his constant guidance, instruction, and encouragement throughout my time in the Chernoff Lab. I also wish to thank Dr. Chernoff, who brought me into the world of biological research and has fostered my learning ever since, along with the other members of his lab who have helped me along the way.

TABLE OF CONTENTS

LIST OF TABLES

LIST OF FIGURES

LIST OF SYMBOLS AND ABBREVIATIONS

Aβ = amyloid beta (peptide)

AD = Alzheimer's Disease

CFP = cyan fluorescent protein

FM = fluorescence microscopy

µL = microliter

mL = milliliter

PCR = polymerase chain reaction

PVDF = Polyvinylidene difluoride

RPM = revolutions per minute

RRM = RNA recognition motif

SDD-AGE = semi-denaturing detergent agarose gel electrophoresis

SDS-PAGE = sodium dodecyl sulfate polyacrylamide gel electrophoresis

U1-70k = U1 small nuclear ribonucleoprotein (70kDa)

YFP = yellow fluorescent protein

YPD = yeast extract peptone dextrose media

CHAPTER 1. ABSTRACT

Alzheimer's disease (AD) is the most common type of dementia and is associated with roughly 500,000 new cases each year (2). AD is associated with the aggregation of two proteins in the brain, A-beta peptide (Aβ) and microtubule associated protein tau (MAPT). Aβ and MAPT are capable of adopting a cross-β fibrous protein structure, which can be reproduced and spread via nucleated polymerization and are termed amyloids. Despite such a broad biological impact of amyloids and prions, the mechanism of their initial formation *in vivo* remains a mystery. In this thesis, I will investigate proteins associated with AD, and the properties of these proteins that control their aggregation. Recent research has indicated that the U1 small nuclear ribonuclear protein 70 (U1-70k) can form detergent-insoluble aggregates in a manner specific to Alzheimer's disease. U1-70k is strongly correlated with Aβ and tau, both proteins known to play a highly important role in the Alzheimer's disease cascade and plaque formation. It has been shown that misfolded forms of U1-70k can sequester natively folded U1-70k proteins and cause them to form insoluble aggregates, a characteristic of amyloids (8). The mechanism behind this conversion remains elusive, however. Our research focuses on determining which domains and combinations of domains of the U1-70k protein are necessary for aggregation, and we also examine its interactions with Aβ. Through plasmid construction, expression, and observation under fluorescence microscopy (FM), we demonstrate that the N(1-99) domain alone cannot induce aggregation, but the C(182-437) domain, combined N and M domains, and M(100-181) domain are capable of inducing aggregation. Further SDD-AGE and Western blot analyses indicate that the aggregates formed by the C(182-437) domain are

detergent-insoluble, while those formed by the N and M domains as well as the M(100-181) domain alone are detergent-soluble. This leads us to hypothesize that the aggregates formed by the M domain are reversible stress granules. Furthermore, the N and M domains also co-aggregate with Aβ, though the C(182-437) domain does not. We also examine tau's suitability as a model in yeast for protein interactions and find that its aggregation is transformant-specific and cannot be cured by Hsp104, a heat shock protein found in yeast cells. We find that wild-type repeat domains of tau, the 244-372 amino acid region, aggregates are detergent-soluble.

CHAPTER 2. BACKGROUND

2.1 Amyloids

A subset of diseases associated with protein misfolding, known collectively as amyloidosis, have become the focus of more research as advances in technology bring us closer to understanding the process of protein folding (9). Every protein in the body must be folded into its correct orientation in order to perform its designated function. An incorrectly folded protein cannot serve its intended purpose, and sometimes these misfolded proteins can take on conformations that have negative consequences for the cell. One category of alternative conformation for proteins is known as the amyloid form. Amyloids are proteins largely composed of cross-β fibril structures, and they are associated with over 50 human diseases, including Alzheimer's disease (AD), Parkinson's disease, and Huntington's disease (9). These proteins aggregate in a disease-specific manner, becoming insoluble and preventing the body from clearing them naturally. They can block off sections of tissues and organs, leading to catastrophic symptoms in a variety of diseases.

2.2 Alzheimer's Disease (AD)

Alzheimer's disease (AD) is a neurodegenerative disease that worsens over time as protein deposits, known as plaques, continue to build in the brain. It is associated with aging and composes 60-80% of dementia cases. The most common symptom is memory loss, though over time, body functions are lost as well, ultimately leading to death. Neuron and synapse loss are additional symptoms of the disease, the pathology of which is marked by neurofibrillary tangles and senile plaques (16). The prevalence of AD is predicted to

quadruple by 2050 (11). The cost of caring for an AD patient in the US is $57,000 per year, and with demographics trending towards more elderly populations, the burden of AD will soon become unsustainable (15). Currently all treatments are purely symptomatic and do not address the underlying mechanics of the disease, largely due to a lack of understanding of its complex processes. Because of this gap in knowledge, the mechanisms of proteins involved with AD pathology have been targeted for potential AD treatments.

2.3 Amyloid Cascade Hypothesis

The amyloid cascade hypothesis is a theory that has dominated AD research for decades and is supported by significant evidence. It posits that the aggregation of the Aβ peptide in the brain is a vital and important step in the disease's progression. Current research seems to point to this step being essential for initiating the disease, but drugs that have targeted Aβ production or aggregation have failed in clinical trials, leading researchers to question whether the whole disease process is driven by Aβ aggregation or whether it is simply one of the first steps in a wide-ranging and complex cascade (15). It is worth noting that the tau protein is also implicated as being 'downstream' of Aβ in the disease cascade, making it the focus of much AD research. Though the role of these two proteins in the disease cascade cannot be overstated, elevated Aβ and tau levels were found in 30-50% of normal, non-AD brains at death (5). This means that the aggregation of Aβ and tau alone cannot sufficiently explain the process of AD. Thus, other proteins and pathways must be examined.

2.4 Aβ Peptide

The amyloid-β (Aβ) peptide has been associated with AD longer than any other protein. The composition and solubility of Aβ aggregates is directly linked to the degree of clinical dementia in AD. The larger protein from which Aβ derives, the β-amyloid precursor protein (APP), is associated with familial early onset AD when mutated. Aβ is derived from APP through sequential cleavage by secretases (16). Three types of secretases cleave APP. The alpha secretase's cleavage prevents Aβ deposition, while cleavage by beta and gamma secretases promotes Aβ production (22). Aβ(1-40) contains 40 residues, while Aβ(1-42) contains 42 due to differential cleavage; Aβ(1-40) dominates amyloids, while both forms are found in senile plaques. It has been hypothesized that the aggregation of Aβ is the 'trigger' for the AD cascade, as discussed earlier. Aβ is also known to interact with a number of other proteins in the brain, including U1-70k.

2.5 snRNP70 (U1-70k) Protein

Recent studies have identified a new protein, U1 small nuclear ribonucleoprotein 70kDa (U1-70k) as having potential amyloid-like properties. The U1-70k protein is known to be involved in the AD protein cascade, and unlike Aβ and tau, its effects have not been heavily studied. U1-70k is a protein component of the U1 snRNP complex in eukaryotes, which in turn is a component of the spliceosome. The spliceosome serves as a molecular machine responsible for splicing introns out of pre-mRNA that have been transcribed to make the final RNA message. After being processed by the spliceosome and undergoing other alterations, the mRNA can then be translated into protein. AD brains show significantly elevated levels of unspliced, non-mature RNA still containing introns (5). This indicates that the intron splicing process may be going unregulated due to U1-70k having lost its function by misfolding. That interpretation could implicate neuronal RNA

processing as playing a more important role in AD pathogenesis than was previously realized. U1-70k also appears to be disease-specific; increased U1-70k presence was observed only in AD brains, not in those with other neurodegenerative diseases, unlike Aβ and tau (5). This high specificity makes it extremely important in studying its relation to AD treatments. Removing the normal function of U1-70k results in increased levels of amyloid precursor protein, which is known to kickstart the AD disease cascade (3). This suggests that U1-70k may actually be upstream of Aβ. Previous studies have shown that U1-70k forms detergent-insoluble aggregates in AD brains, a characteristic typical of amyloids (8). These U1-70k aggregates appear and spread across the brain in a very similar pattern to the spread of tau aggregates (3). Similar aggregates seen in mild cognitive impairment (MCI), the early-stage precursor to symptomatic Alzheimer's disease, suggest that the aggregation and amyloidogenesis of U1-70k occurs early in the disease cascade, making it an ideal target for preventative treatment (3). It should also be noted that another study has shown that in AD, U1-70k is N-terminally cleaved to a size of 40kDa. The N40K fragment has been shown to have toxic effects on neurons, suggesting this protein may play a role in neurodegeneration of AD patients (3).

2.6 Tau Protein

The tau protein is an important protein of interest in AD as well. This natively unfolded protein is normally found abundantly in the central nervous system, where it stabilizes microtubules (16). It is associated with disease pathologies other than AD, such as FTDP-17; these are collectively known as tauopathies. Due to its unfolded nature, it has a variety of isoforms it can take, as well as other proteins it can interact with. Normally tau is highly soluble, but it can aggregate when its short hydrophobic motifs form β-sheet

structures (16). Tau's aggregates are toxic to the brain, and it is hypothesized that they are triggered by Aβ's 'upstream' aggregation.

2.7 Goals

The main question about the role of U1-70k in AD is the same as for many other proteins involved in amyloid diseases: it is still unknown exactly how normal, soluble U1-70k proteins actually become insoluble aggregates. Diner *et.al.* 2014 theorized that the process accelerates by means of aggregated U1-70k surrounding and sequestering natively folded U1-70k proteins, preventing them from functioning and thus forming larger detergent-insoluble aggregates (5). However, this still does not answer the question of how the aggregates appeared in the first place. The protein's domains, which contain its structural information, have been suspected to play a role in its change of function. It has been shown that the C-terminus of U1-70k, which contains two disordered low complexity domains, LC1 and LC2, is necessary and sufficient for U1-70k aggregation (5). The ability to form aggregates was attributed to the low amino acid diversity of those LC subunits, but it was not explained how amino acid composition could have this effect. Additionally, failing to sufficiently test the other domains of the protein presents an incomplete picture of its properties.

Through investigating the other domains, we can determine if they too have areas of low complexity and high disorder, as Diner first proposed (5). If they do not, this would suggest that factors other than complexity play a role in causing aggregation. Our results thus far show that the combined N and M domains are also capable of inducing aggregation, which seems to conflict with the results of Diner and Hales (14). In our experiments, we

will continue to use yeast as a model organism for mammalian diseases, as yeast are also plagued by amyloids, known as yeast prions, making them a useful tool for the study of human disease (10).

It is also essential to study the interactions of U1-70k with the two most major proteins implicated as part of the AD cascade: Aβ and tau. By examining the relationship between these proteins and U1-70k, we can work towards determining the location of U1-70k in the AD cascade. Whether it is "upstream" or "downstream" from Aβ may have considerable consequences for AD research.

Previously, we had only observed aggregation in the combined NM(1-181) domains. We extended our investigation to other domains and combinations of domains within U1-70k in order to determine which are necessary for amyloid formation to occur. Determining which domains are responsible for aggregation will not only aid in targeting U1-70k for treatment, but it can aid in the understanding of what exactly causes the protein to aggregate, allowing for more targeted and effective treatments of AD.

In order to study the amyloidogenic properties of U1-70k, we have cloned domains of the human U1-70k gene fused to the yellow-fluorescent protein (YFP) into a yeast (*S. cerevisiae*) shuttle plasmid, under an inducible copper (P_{CUP}) promoter. We now aim to test the isolated N, M, and C domains to determine which domains are capable of inducing aggregation and, of these, which aggregates are detergent-insoluble. We also examine the interactions of the NM and C domains with Aβ through colocalization and assess whether tau in yeast can function as an accurate model for tau in other organisms, in preparation for

future experiments involving tau. Finally, we characterize tau's aggregations with SDD-AGE and SDS-PAGE.

CHAPTER 3. MATERIALS AND METHODS

3.1 Yeast Media

Yeast were grown at 30ºC. Rich yeast medium (YPD) was constructed from 2% peptone, 2% dextrose, and 1% yeast extract. Other media were built that lacked one or two amino acids, to be used as screens for plasmids with those markers. Those media were labeled according to the amino acid(s) they lacked; for example, -leu media was missing leucine. Yeast media could either be solid (with agar, on plates) or liquid (without agar, in flasks or bottles), depending on its intended purpose.

3.2 Plasmid Construction

An existing plasmid, P_{CUP}-PHC3-YFP, (made by our collaborator Anastasia Grizel) was used as a backbone for all newly constructed U1-70k plasmids. The new plasmids were P_{CUP}-U1-70kN(1-99)-YFP, P_{CUP}-U1-70kM(100-181)-YFP, P_{CUP}-U1-70kNM(1-181)-YFP, and P_{CUP}-U1-70kC(181-437)-YFP. For construction, the vector plasmid P_{CUP}-PHC3-YFP was incubated with the restriction enzymes BamHI and Xba1 to remove *PHC3*, and to place in domains of U1-70k flanked by the same enzymes sites inserted using PCR. A simplified view of the plasmids is shown in Figure 1. All digests were run on an agarose gel to separate out the desired fragment, which was cut out of the gel and purified with a Monarch © DNA gel extraction kit. DNA fragments were ligated using T4 DNA ligase, resulting in the desired plasmid construction (U1-70k domains fused to YFP under the P_{CUP} promoter).. All plasmids were verified by sequencing. For MAPT, P_{GPD}-Tau(244-372)-YFP was given to us by our collaborators at Saint Petersburg University, Russia..

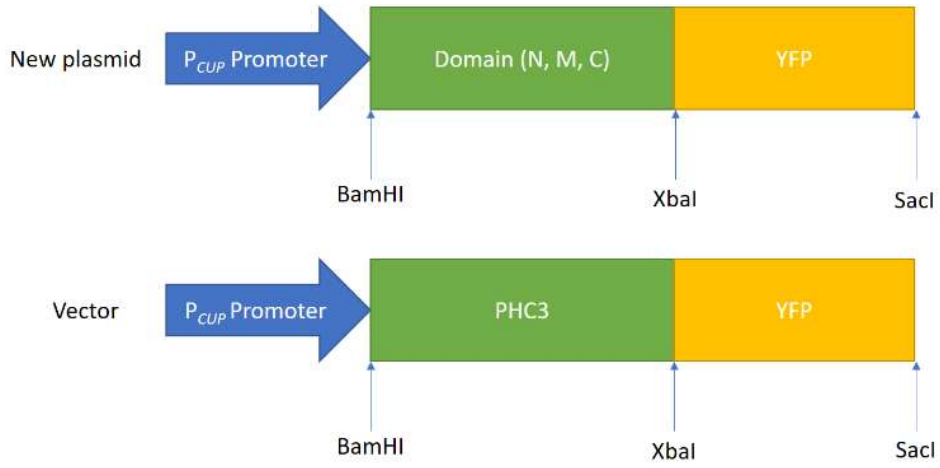

Figure 1. Diagram of plasmid construction. This example compares a newly created plasmid to the vector it was derived from. Each plasmid included an inducible copper (P_{CUP}) promoter and a fluorescent protein (YFP). Arrows indicate recognition sites for restriction enzymes.

3.3 Bacterial Transformation

To transform plasmids into *Escheria coli* (*E. coli*) bacteria, competent cells (DH5α) were first thawed on ice. 5 µL of plasmid DNA were added to a microfuge tube along with 50 µL of competent cells. The cells and DNA were mixed by flicking the tube, which was then placed on ice for 30 minutes. After this, the mixture was heat-shocked for 45 seconds at 42ºC, then placed on ice again for 2 minutes. 950 µL of fresh room temperature super optimal broth with catabolite repression medium (SOC medium) was added to the tube. SOC was prepared from super optimal broth (SOB), magnesium chloride, and glucose. The mixture was then incubated at 37ºC for an hour with shaking. During this time, selection plates of media were warmed to 37ºC. The cells were mixed by flicking and diluted if necessary. 50-100 µL of the cell mixture was spread onto each plate using glass beads, and the plates were incubated overnight at 37ºC.

3.4 Transformation into Yeast

Yeast cells were transformed in accordance with the protocol described by Gietz *et al.* (13). To transform the plasmids into yeast, a pre-culture was grown in 10 mLs of YPD. The cells were then diluted into a 50 mL flask of fresh YPD and incubated for 2 hours. The culture was then transferred to a sterile Oakridge tube and centrifuged at 3,000 RPM for 10 minutes. The supernatant was poured out, and the pellet was washed with 10 mL of Tris-EDTA (TE) buffer. The pellet was resuspended in 10 mLs of lithium acetate Tris-EDTA buffer (LiAc-TE). Cells were incubated with LiAc-TE with shaking for 1 hour. Cells were then centrifuged and resuspended into 1mL of LiAc-TE. For the transformation reaction, 100 µL of cells (per transformation) were transferred to a microfuge tube and incubated for 30 minutes with 10 µg of DNA (the transforming plasmid) and 20 µg of carrier DNA. A tube with no DNA was used as a control. After the 30 minute incubation, 700 µL of lithium acetate polyethylene glycate Tris-EDTA buffer (LiAc-PEG-TE) was added to each tube , followed by a 1 hour incubation. The samples were then heat-shocked for 6 minutes at 42ºC, then placed at 4ºC overnight. The next day, the samples were centrifuged at 3000 RPM for 2 minutes. The supernatant was poured out, and the cells were resuspended in 250 µL of water. 250 µL of each sample were then pipetted onto plates with selection for the plasmid marker and allowed to grow for 3-4 days at 30ºC.

3.5 Fluorescence Microscopy

The yeast cultures were diluted to OD_{600} = 0.5. Protein expression was induced with 4 different concentrations of copper sulfate: 0 µM, 100 µM, 200 µM, and 300 µM. The yeast cells were centrifuged at 3000 RPM for 10 minutes. The pellet was washed with 500

μL of water and transferred to a microfuge tube, where it was again centrifuged at 3000 RPM for another 10 minutes. If necessary, the cells were diluted in another centrifuge tube with a 3:1 ratio of water to cells. Each mixture was then spread on a glass microscopy slide with a pipette tip, dried under a hood, and covered with a glass slide with 10 μL of water added. The slides were mounted with fast-drying nail polish. Starting from the 0 hour time point (0 hours after the induction), the slides were analyzed using a Olympus BX41 microscope with an Olympus DP-71 camera from Chroma Technology Corporation. Photos were taken under white light and using the excitation wavelength for the yellow fluorescent protein. This process was completed for a total of 6 time points for each plasmid: 0 hours, 3 hours, 6 hours, 24 hours, 48 hours, and 72 hours. The images were analyzed with ImageJ, and percentage aggregation was determined by counting the number of cells containing aggregates as a percent of the total number of cells containing the plasmid.

3.6 SDS-PAGE and Western blotting

For SDS-PAGE (sodium dodecyl sulfate polyacrylamide gel electrophoresis) and analysis with a Western blot, cells were harvested at the 6 hour time point and lysed with silica beads. The protein was harvested and incubated with 4x loading buffer (240 mM Tris-HCl pH 6.8, 8% SDS, 40% glycerol, 12% 2-mercaptoethanol and 0.002% bromophenol blue) at room temperature for 10 minutes. The samples were then loaded into a 10% SDS-polyacrylamide gel in Tris-Glycine-SDS running buffer (0.1% SDS, 192 mM glycine, 25 mM tris, pH 8.3) and run on the gel. After the gel was run, a PVDF membrane was cut to the same size as the gel, along with two pieces of Hybond-ECL nitrocellulose membrane. A stack was prepared, containing a sponge, filter paper, the gel, the membrane,

another layer of filter paper, and another sponge. The stack was placed in the Transfer-Blot (Bio-Rad) and covered with TAE/SDS buffer. The transference was run for 1 hour at 100 volts. The membrane was then pre-blocked with 5% non-fat milk and probed with an antibody specific for YFP. The membrane was then washed, and excess reagent was removed. It was then wrapped in plastic wrap, put in a case to protect it from light, and imaged by chemiluminescence using x-ray film.

3.7 SDD-AGE

The SDD-AGE (semi-denaturing detergent agarose gel electrophoresis) procedure was carried out in much the same way as the SDS-PAGE, except that the samples were run in a 1.8% Tris-Acetate EDTA (TAE) agarose gel with 0.1% SDS instead of the polyacrylamide gel, and a Whatman membrane was used rather than the Hybond-ECL one. All other steps were the same. The kinetics of the proteins being run on the gel are shown in Figure 2.

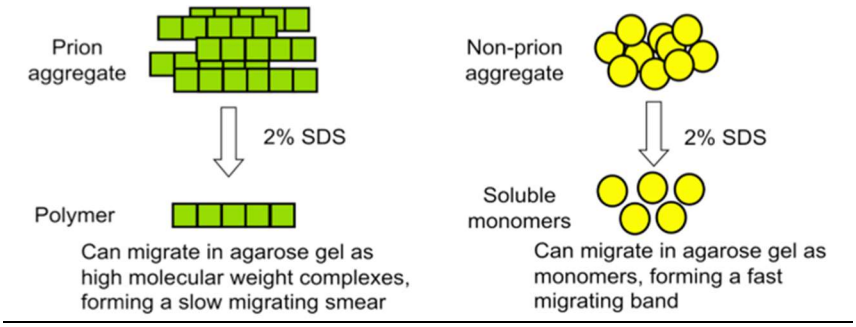

Figure 2. Kinetics of aggregate formation. A graphic displaying the differences in how polymers and monomers move on a SDD-AGE gel. Polymers (in this case, insoluble aggregates) will appear as dark, dense, slow-moving smears on a Western blot, whereas soluble monomers will appear as lighter, fast-moving bands.

3.8 Boiled Gel

The boiled gel process was conducted in the same way as the SDS-PAGE, except that rather than boiling protein samples prior to loading, they were loaded without being boiled and run for roughly 40 min in the gel. Electrophoresis was then halted, and the wells were filled with fresh acrylamide to retain any aggregated protein that was still in the wells. After the polyacrylamide had dried, the gel was boiled in a water-tight bag for 20 minutes. Once it had cooled, it was returned to the electrophoresis box, and the electrophoresis process was continued. The Western blot was performed in the same way as described for SDS-PAGE.

3.9 Yeast Mating

The yeast pre-cultures were grown in media selective for their respective plasmid, along with two mating type check strains in YPD. The pre-cultures were streaked across a new YPD plate in two lines. Cells from the mating type check strains were then streaked perpendicular to the first line, then the plates were incubated overnight. The following day, the plates were velveteened to drop-out media selective for the markers of both plasmids to screen for the diploids. The drop-out media plates selective for diploids were then incubated for 2 days to allow colonies to grow. An overview of how this procedure was performed for the mating of U1-70k and Aβ is shown in Figure 3.

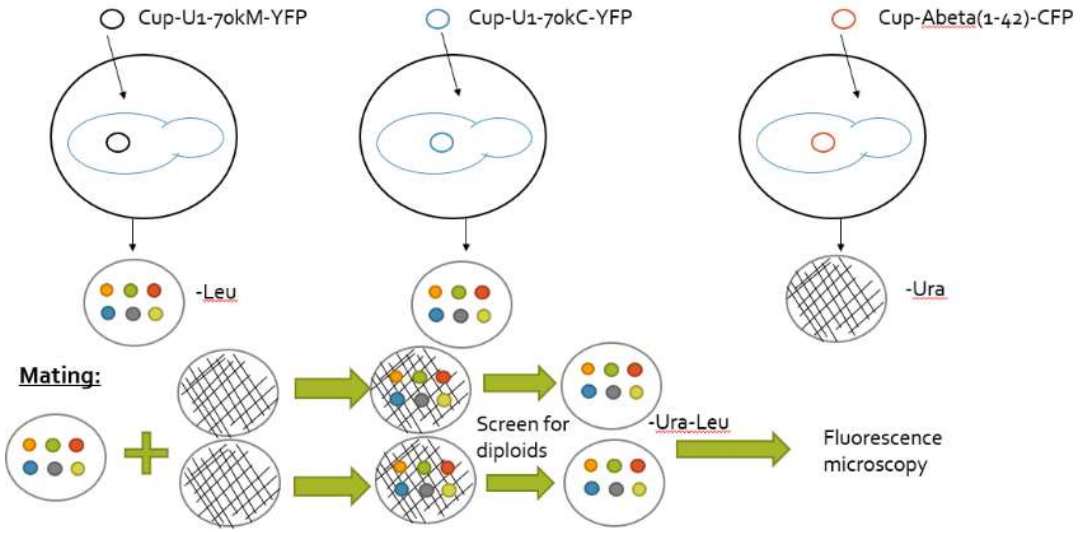

Figure 3. Yeast mating experimental design. This figure shows how the diploid strains containing Aβ(1-42) and U1-70kNM(1-181) or U1-70kC(182-437) were created through yeast mating. The plasmids containing U1-70k have a *LEU2* marker, and the Aβ plasmid has a *URA3* marker, allowing them to be screened with -URA-Leu plates to select for diploids.

3.10 Colocalization

For colocalization studies, plasmids were constructed according to the procedure described in 2.2.1 with differing genes for fluorescent proteins. In this case, cyan fluorescent protein (CFP) and yellow fluorescent protein (YFP) were to distinguish between the two proteins of interest. The plasmids were then transformed into yeast according to the procedure in 2.4, mated as described in 2.8, and imaged as described in 2.5. One image was taken using the filter with the emission wavelength for CFP and one with the filter with the emission wavelength for YFP filter, as well as one brightfield image. The CFP and YFP images were merged into one using software provided by Olympus, and

the resulting image was analyzed with ImageJ to determine what percentage of cells expressing both CFP and YFP foci were expressing them in the same location in the cell.

CHAPTER 4. CHARACTERIZING THE DOMAINS OF U1-70K

4.1 Introduction

The U1 small nuclear ribonucleoprotein-70k (U1-70k) is a spliceosome component of the U1 snRNP. It has 3 domains: the N-terminus, the M domain containing the RNA recognition motif (RRM), and the C domain. The C domain is known to contain 2 regions of low amino acid complexity (5) thought to be essential to its aggregation. One of those low-complexity regions has been shown to interact with tau from AD brains but not from other tauopathies, indicating that it may be disease-specific (14). We hypothesize that the C domain controls the aggregation of U1-70k and that its aggregates are detergent-insoluble, like those found in AD brains.

4.2 Results

Our results indicate that the U1-70kN(1-99) domain does not form aggregates at any time point or concentration of copper sulfate, as seen in Table 1.

Table 1. Percent aggregation of Cup-U170kN-YFP over time. The N domain shows only diffuse fluorescence under FM and does not form aggregates at any time point or concentration of $CuSO_4$.

Time (hours)	Average Percent Aggregation
0	0
3	0
6	0
24	0
48	0
72	0

We also found that the U1-70kNM(1-181) domain is able to form fluorescent foci without the presence of the C domain, as seen in Figure 4. Two SDD-AGE analyses were performed on separate samples of U1-70kNM(1-181) proteins, with conflicting results, as can be seen in Figure 5. The first seemed to indicate that the NM domains could form detergent-insoluble aggregates, while the second showed that these aggregates were in fact detergent-soluble. Another cleaner SDD-AGE will be performed to clear up any confusion surrounding the nature of these aggregates.

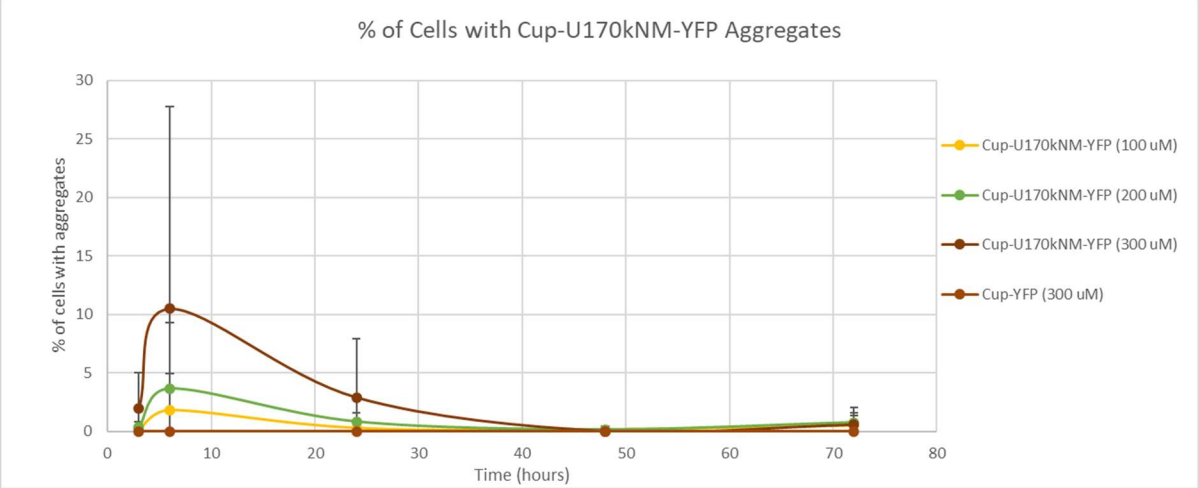

Figure 4. Percent aggregation of Cup-U170kNM(1-181)-YFP over time. Cup-U170kNM(1-181)-YFP forms fluorescent foci over time, peaking at 6 hours post-induction with $CuSO_4$ and decreasing to nearly 0% aggregation by 72 hours. All error bars, unless otherwise indicated, represent standard deviation.

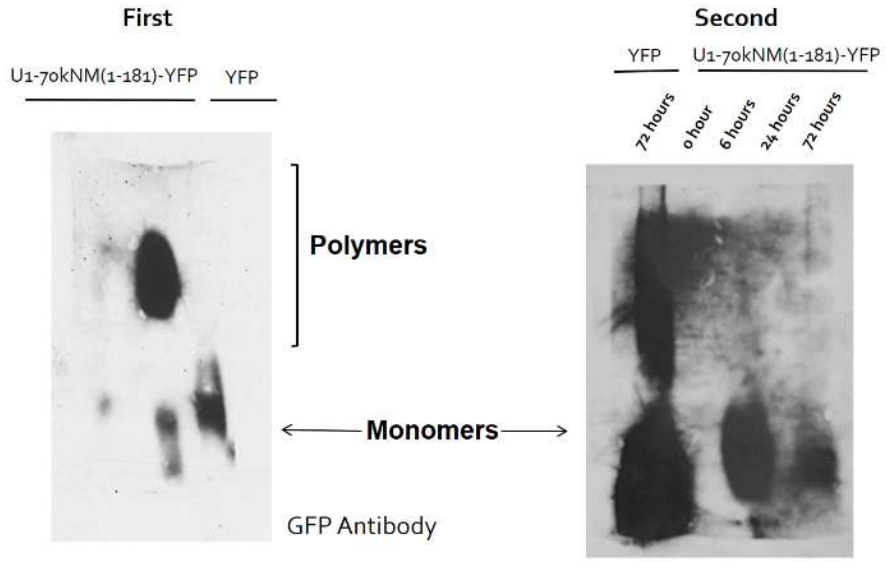

Figure 5. SDD-AGE results for U1-70kNM. The first SDD-AGE (left) seems to indicate that U1-70kNM(1-181) aggregates are detergent-insoluble, but the second one (right), which includes protein samples from 4 different time points, shows them moving as soluble monomers. These experiments were conducted using two different transformants.

Our results indicate that the U1-70kC(182-437) domain is able to form fibril-like aggregates in a [psi$^-$][pin$^-$] strain when over-expressed, as seen in Figure 6. The aggregates formed by this domain are detergent-insoluble, as shown by the SDD-AGE in Figure 7. They travel as a polymer rather than a monomer, forming a slowly migrating blur on the membrane, as displayed in Figure 2.

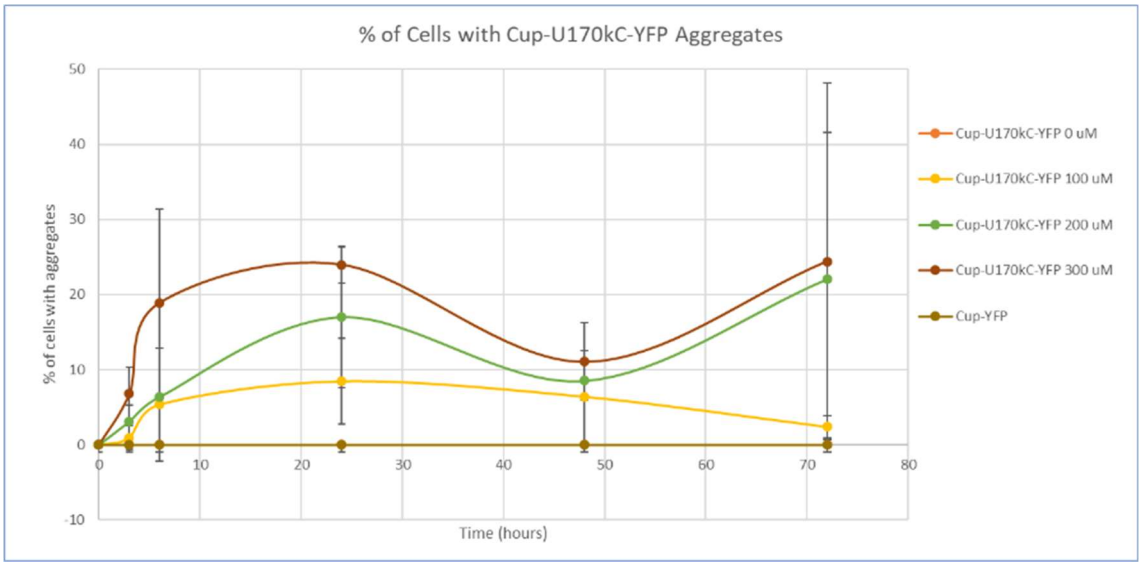

Figure 6. Percent aggregation of P*CUP*-U170kC(182-437)-YFP over time. P*CUP*- U170kC(182-437)-YFP forms fluorescent foci over time. Aggregation remains relatively constant after 6 hours apart from a slight dip at 48 hours. The aggregates are still significantly present at 72 hours post-induction.

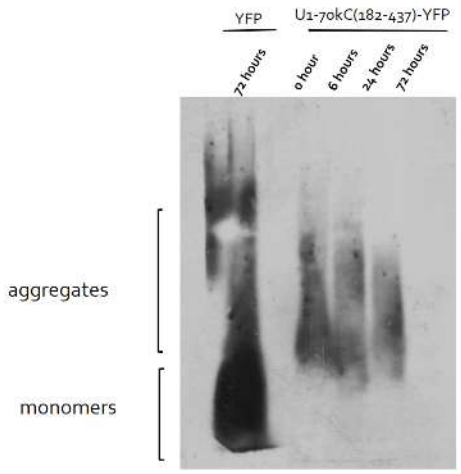

Figure 7. SDD-AGE results for P*CUP*-U170kC(182-437)-YFP. P*CUP*-U170kC-YFP forms detergent-insoluble aggregates, as can be seen in the 6, 24, and 72 hour lanes. No

protein is present in the 0 hour lane as induction had just begun at that point. Slow-moving polymers are present in all other lanes.

As can be seen in Figure 8, results for the M domain alone indicate that it too can cause the appearance of fluorescent foci, as we had predicted, indicating the the aggregation of the NM(1-181) fragment may be controlled by the M domain. The Western blot in Figure 9 shows that these types of aggregates formed by the M domain are in fact detergent-soluble, like those formed by the N and M domains together. The control plasmids containing just P_{CUP}-YFP did not aggregate in any experiment, displaying the necessity of U1-70k domains in aggregation. It is also worth noting that for the NM and M domains, the percentage of cells displaying aggregates peaked at the 6 hour mark and gradually fell off to a consistent 0% at the 72 hour mark. This pattern was not consistent for the C domain, which kept up a relatively stable percentage aggregation over time.

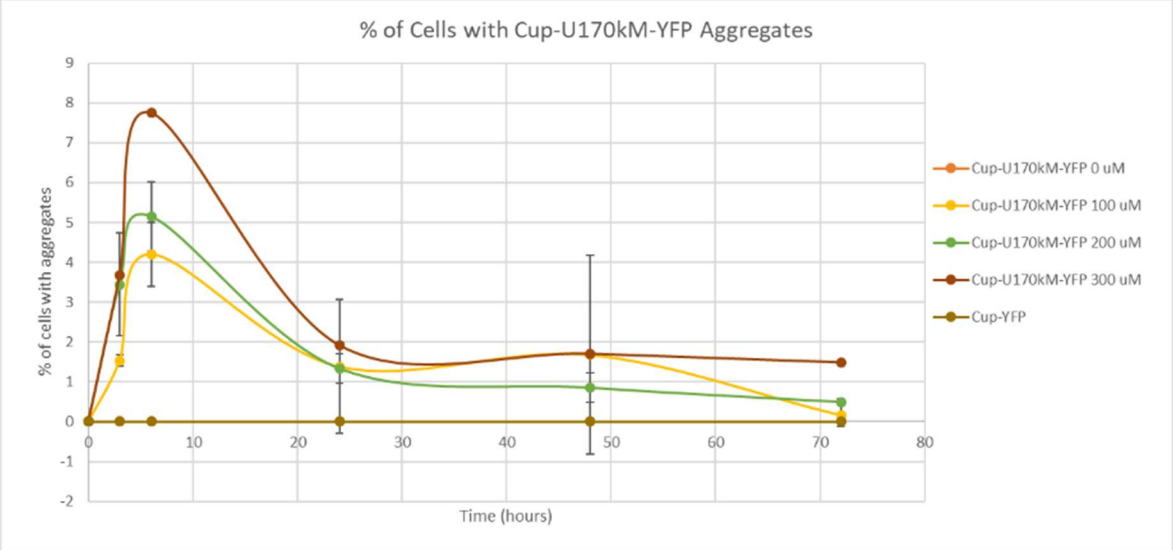

Figure 8. Percent aggregation of P_{CUP}-U170kM(100-181)-YFP over time. P_{CUP}-U170kM-YFP forms fluorescent foci over time, peaking at 6 hours post-induction with

copper sulfate and decreasing to nearly 0% aggregation by 72 hours, just as was seen in P_{CUP}-U170kNM(1-181)-YFP.

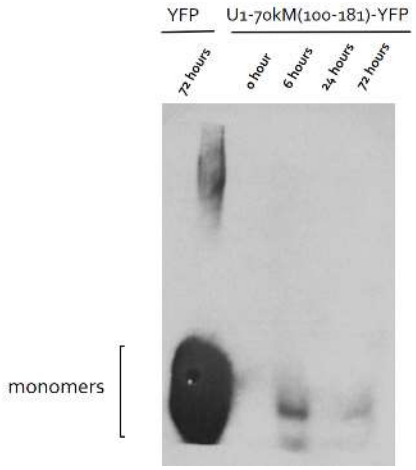

Figure 9. SDD-AGE results for P_{CUP}-U170kM-YFP. The proteins only run as monomers. The 0 hour lane shows no protein presence due to induction having just begun. The 24 hour lane seems to be blank, but this may be due to the amount of protein loaded. The strongest protein presence is at the 6 hour time point, in accordance with the FM results.

We also performed colocalization studies between aggregating domains of U1-70k and Aβ in order to determine if the proteins are interacting. Colocalization of the aggregates would imply a relationship between the proteins; namely, that the aggregation of Aβ would be causing the aggregation of U1-70k. It was found that P_{CUP}-U1-70kNM(1-181)-YFP was able to colocalize with P_{CUP}-Aβ(1-42)-CFP at the tested 6 and 24 hour time points, as can be seen in Figure 10. The aggregates themselves can be seen in Figure 11. However, P_{CUP}-U1-70kC(182-437)-YFP did not colocalize with P_{CUP}-Aβ(1-42)-CFP, as shown in Figure 12. The aggregates remained separate and were not overlaid, as shown in Figure 13.

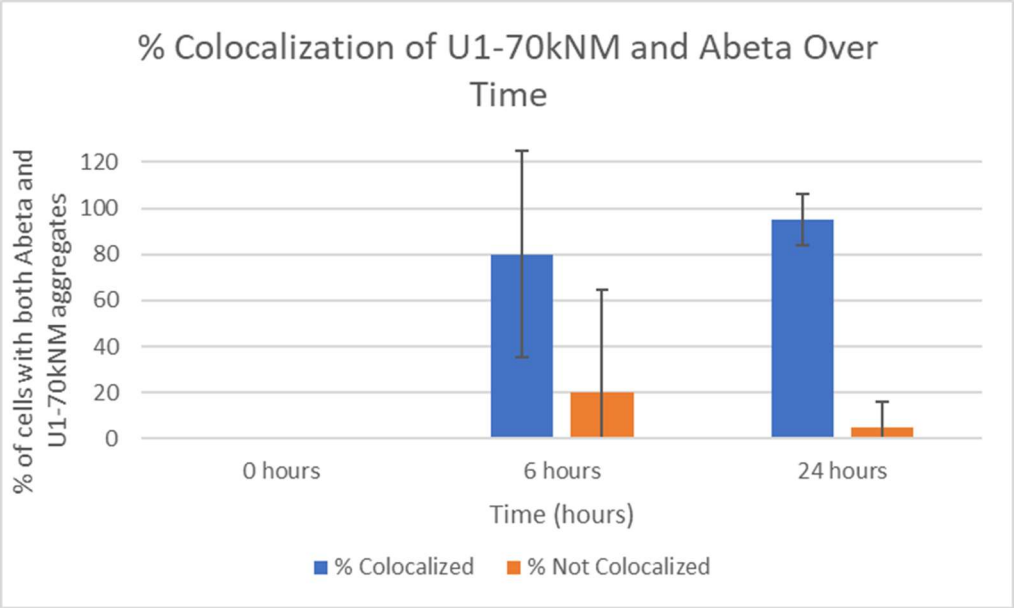

Figure 10. Colocalization of P_{CUP}-U1-70kNM(1-181)-YFP and Cup-Aβ(1-42)-CFP over time. The NM domain of U1-70k colocalizes clearly with Aβ(1-42). By 24 hours, nearly all of the cells expressing both CFP and YFP-tagged aggregates (Aβ(1-42) and U1-70kNM(1-181) respectively, can be seen as colocalized.

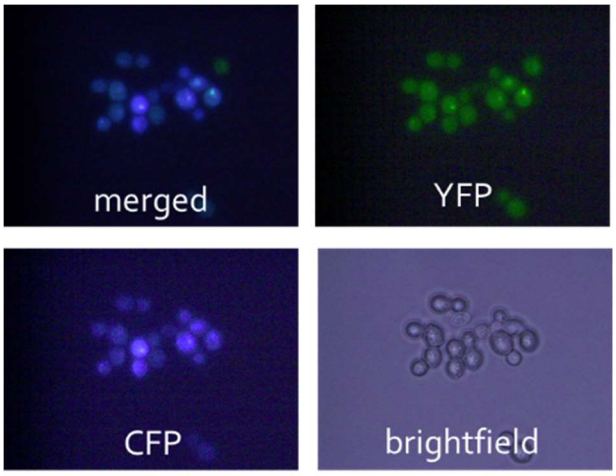

Figure 11. Fluorescence microscopy results of P_{CUP}-U1-70kNM(1-181)-YFP and P_{CUP}-Aβ(1-42)-CFP colocalization at 6 hours. Pictures were taken under cyan light

(CFP), yellow light (YFP), and white light (brightfield). The CFP and YFP images were overlaid to create the "merged" image, allowing us to determine whether the aggregates were colocalized. Nearly all cells expressing both types of aggregates displayed colocalization.

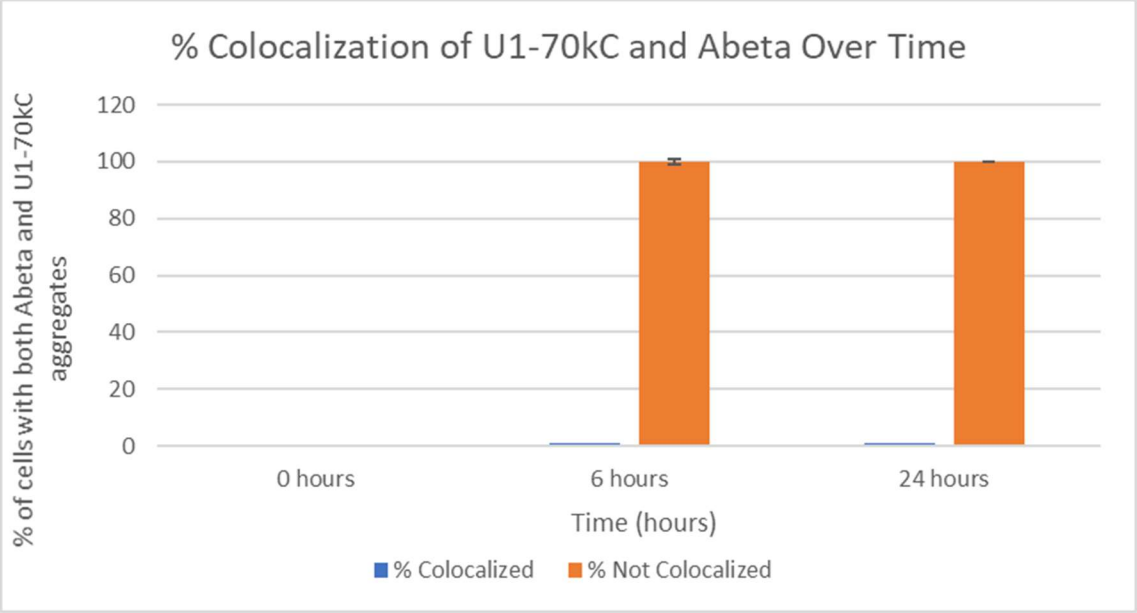

Figure 12. Colocalization of Cup-U1-70kC-YFP and Cup-Aβ-CFP over time. The C domain of U1-70k does not colocalize with Aβ(1-42) at any time point. Even samples with up to 14 aggregates did not have any CFP and YFP aggregates in the same location of the same cell.

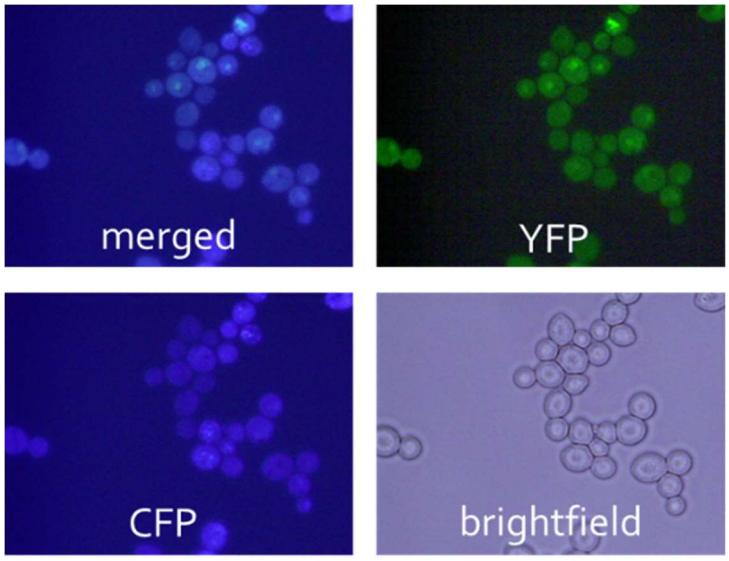

Figure 13. Fluorescence microscopy results of P$_{CUP}$-U1-70kC(182-437)-YFP and Cup-Aβ(1-42)-CFP colocalization at 6 hours. The aggregates of each type did not colocalize, usually manifesting in separate cells or, when they did occur in the same cell, segregating to opposite ends of the cells.

4.3 Discussion

The over-expression of U1-70kN(1-99) results in diffuse fluorescence. This alters our initial hypothesis that the N-domain (an unstructured domain) was causing the aggregation of the U1-70kNM domain. These results match findings by Diner *et al.* suggesting that the N domain cannot aggregate on its own, despite containing an unstructured domain. The results of the C domain support existing findings indicating the aggregation-inducing abilities of that domain. The fact that the N and M domains combined can cause aggregation of some sort would indicate that the C domain is not actually necessary to cause aggregation. Because the NM domains aggregated together, but the N

domain did not aggregate by itself, we hypothesize that the M(1-181) domain is responsible for aggregation of the NM(1-181) domain.

The results of the SDD-AGE analyses indicate that only the C(182-437) domain is capable of forming detergent-insoluble aggregates. This is in agreement with previously published data by Diner *et al*. This is in assumption that the second SDD-AGE for the NM(1-181) domains is correct, which suggests that the aggregates formed by the M(100-181) domain may be of a different type than those formed by the C domain. For now, our results seem to support the second SDD-AGE, as the aggregates formed by the M(100-181) domain alone were soluble and the N(1-99) domain cannot form aggregates. It follows to conclude that, until we can perform another SDD-AGE, the aggregates formed by the NM(1-181) domains together are likely soluble. Our evidence as of now seems to point to the aggregations of the M(100-181) domain actually being stress granules. Stress granules are aggregations of proteins and RNA that can occur when the cell is under stress. Unlike amyloids, they are reversible and can dissociate over time. They can be caused by a number of factors, including heat, cold, and overexpression of proteins (18). It should be noted that percentage aggregation of the C(182-437) domain remains relatively constant over time and is still very much present at 72 hours, while for the NM(1-181) and M(100-181) domains, aggregation peaks at 6 hours and decreases after that to almost 0% by 72 hours. If these aggregations were stress granules, it would explain their disappearance over time, as stress granules can dissociate naturally. It would also account for their detergent-solubility, as opposed to the aggregations formed by the C domain. U1-70kNM's colocalization with Aβ could be due to Aβ's aggregation triggering the formation of stress granules in the same location as Aβ. It is also important to recall that the M domain of U1-

70k is the RNA-binding domain, which could be related to the formation of these RNA-based stress granules.

4.4 Conclusions

- Of the domains of U1-70k, 2 out of 3 are capable of inducing aggregation on their own: the M(100-181) and C(182-437) domains. Only the N(1-99)-terminus domain is incapable of inducing aggregation.
- The aggregates formed by the M(100-181) and C(182-437) domains are likely different types of aggregates, with the M(100-181) domain potentially forming stress granules and the C(181-437) domain forming fibril-like detergent-insoluble aggregates similar to the ones found in AD. This would correlate with the findings of Diner *et al.* who state that the C domain alone is necessary and sufficient for detergent-insoluble aggregation.
- The aggregates formed by the NM(1-181) domains of U1-70k can colocalize with those formed by Aβ, while the aggregates formed by the C domain cannot.

4.5 Future Directions

The next step in the investigation of U1-70k will be to construct a plasmid containing all 3 domains of U1-70k (i.e. its full length) and test it as we have tested the previous domains for aggregation and detergent-insolubility. To answer the question about the nature of the M domain's aggregates, we intend to run colocalization tests of Cup-U1-70kM-YFP and Pub1, a marker for stress granules. Colocalization tests will also be run between Cup-U1-70kM-YFP and Cup-Aβ(1-42)-CFP to determine if colocalization still occurs without the N domain.

CHAPTER 5. ANALYZING TAU'S AGGREGATIONS

5.1 Introduction

Microtubule-associated protein tau (MAPT, or tau) is a natively unfolded protein usually found in one of 6 isoforms formed by alternative splicing. It is located in the central nervous system, where it stabilizes microtubules in the brain. Under normal conditions it is soluble, but in certain cases it can become insoluble and form β-sheet structures as it aggregates. Tau became associated with AD after it was discovered that the accumulation of amyloidogenic tau in the human brain correlates with the cognitive decline seen in AD and other tauopathies (19). When tau begins to nucleate, it loses its native function, and the microtubules it had previously stabilized become disorganized, forming neurofibrillary tangles (NFTs) (20). Because tau has proved to be dangerous in humans, we wish to determine if tau can be used in yeast as an accurate model for protein interactions and determine if its aggregates are detergent-insoluble. Yeast have proven to be an invaluable tool in the study of protein aggregation, with a lot of our understanding coming from in vitro and microcellular models. We hypothesize that tau will behave similarly in yeast as it does in humans. We also hypothesize that the Hsp104 protein will be able to cure the aggregates formed by tau. Hsp104 is a heat shock protein that appears to be able to cure some tau aggregations in certain strains of yeast.

5.2 Results

We first assessed the validity of the tau model in yeast and found that the repeat domain of tau, the 244-372 amino acid domain, could aggregate in any of the prion-free,

prion-containing, or diploid strains that we tested it in. However, we found that the repeat domain of tau's aggregation was transformant-specific, as can be seen in Figure 14. Since the aggregation properties of the repeat domain of tau are transformant specific, a representative transformant that did not aggregate was used for subsequent experiments and will be referred to as the non-aggregation strain. Two representative transformants were selected that did aggregate and were used in experiments and will be referred to as the aggregation strains #1 and #2.

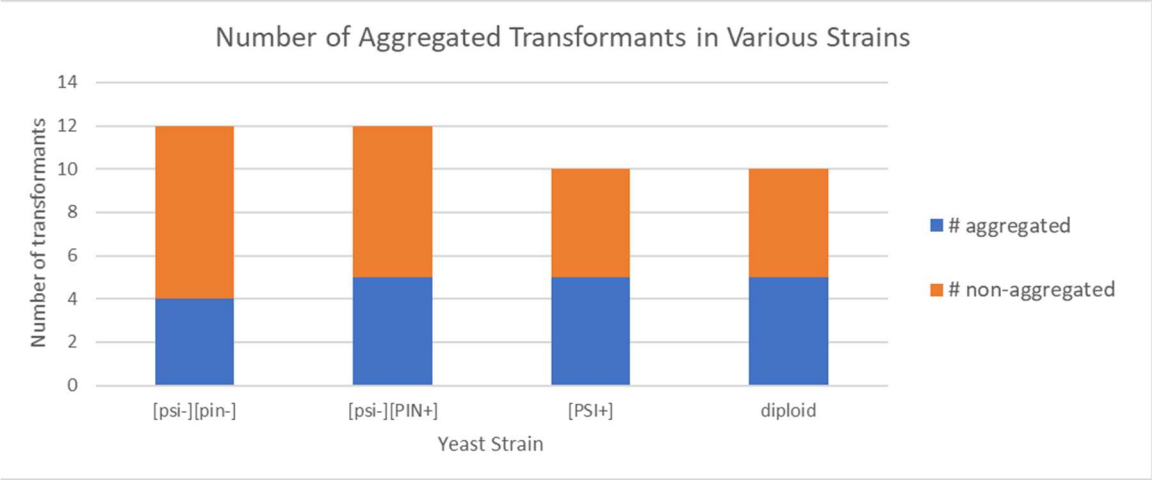

Figure 14. Tau aggregation is transformant specific in various yeast strains. The repeat domain of tau can aggregate in a prion-free strain ([psi$^-$][pin$^-$]), in a strain with the prion caused by the Rnq1 protein ([psi$^-$][*PIN*$^+$]), in a strain with the Sup35 prion ([*PSI*$^+$]), and in a diploid strain. It was essential to prove that tau can aggregate in a diploid strain, as it we would look for aggregation of tau in conjunction with Hsp104, which would be done via mating.

We then tested three strains of tau- two aggregating strains and one non-aggregating strain, as well as a Cup-YFP control- to determine if their aggregates were detergent-

insoluble. SDS-PAGE results with a GFP antibody showed that all the strains and the control were being expressed, while the loading control with a RPL3 antibody showed that the gel lanes were evenly loaded with the samples. Figure 15 shows the results of the SDD-AGE. It was observed that all the proteins in both the aggregating and non-aggregating strains traveled as monomers.

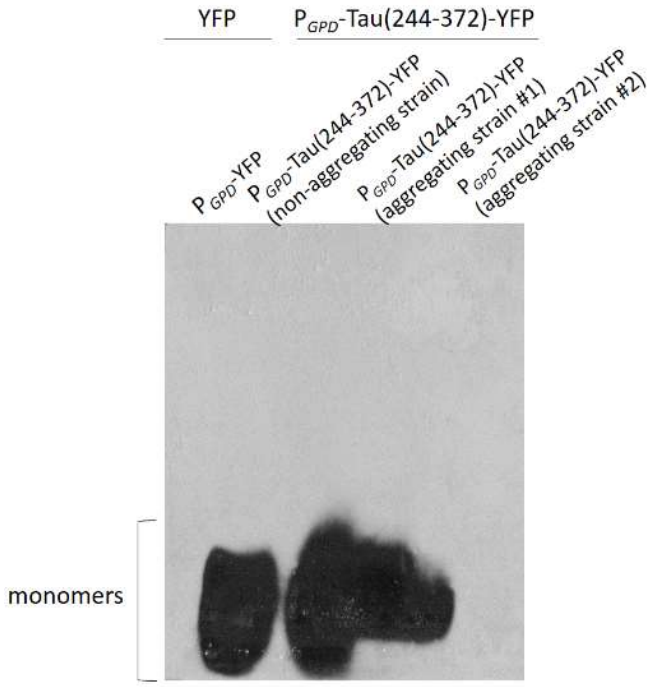

Figure 15. SDD-AGE results for P$_{GPD}$-Tau(244-372)-YFP. The SDD-AGE shows that all proteins traveled as monomers, leaving no smears indicating high molecular weight aggregates. The results of the aggregating strains match those of the non-aggregating strains, indicating that the aggregates are not detergent-insoluble.

The results of the boiled gel match the results of the SDD-AGE; as seen in Figure 16, the unboiled samples match the boiled samples in molecular weight. There are no high

molecular weight aggregates that would indicate detergent insolubility. Therefore, all these aggregates must be composed of soluble monomers.

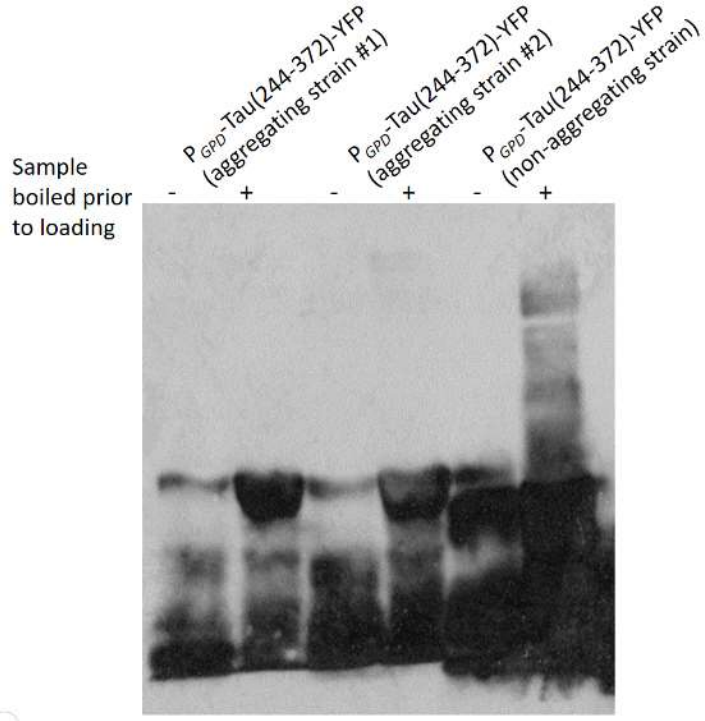

Figure 16. Boiled gel results for P_{GPD}-Tau(244-372)-YFP. Apart from an unclear smear in the last lane, there appear to be no differences between the boiled and unboiled samples, suggesting that no high molecular weight aggregates are present.

Figure 17 shows the results of the SDS-PAGE conducted on the aggregating and non-aggregating tau samples. All the proteins are being expressed, but the same plasmid seems to be expressed differently in its aggregating and non-aggregating forms. This leads us to hypothesized, based off the results below, that the aggregating form has been phosphorylated, leading to the difference in molecular weight. Figure 18 displays the differences between aggregating and non-aggregating tau strains under FM.

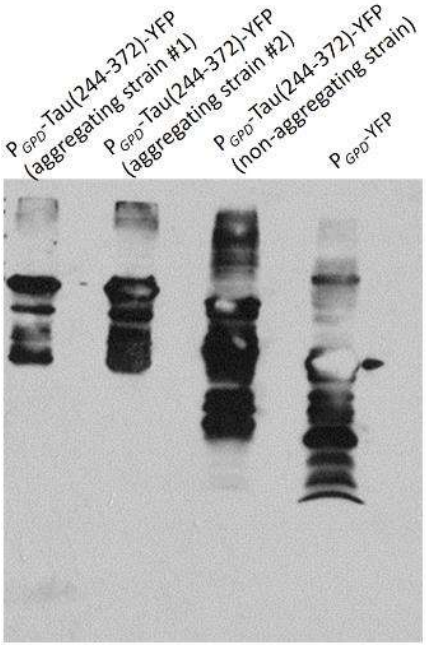

Figure 17. SDS-PAGE results for P_{GPD}-Tau(244-372)-YFP. The same plasmid is expressed differently between the aggregating and non-aggregating strain. The aggregating strains appear to have a higher molecular weight than the non-aggregating strains, possibly indicating that phosphorylation is occurring in the aggregating strains.

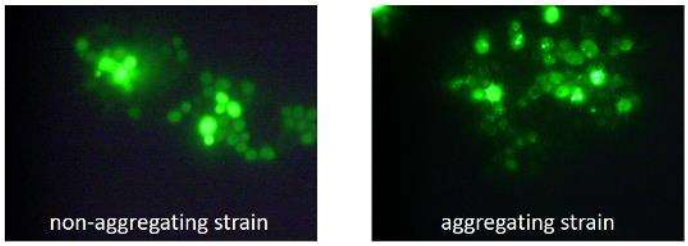

Figure 18. Fluorescence microscopy images of tau samples. Non-aggregating strains display no tau aggregates, whereas aggregating strains often display multiple aggregates per cell.

Through yeast mating, we created diploid strains containing either the non-aggregation strain on aggregation strain of tau along with the plasmid P_{GPD}-Hsp104. We

found aggregates only in the aggregating strains, as expected, and we found that Hsp104 does not significantly cure tau aggregations. Aggregating strains with Hsp104 experienced a slight decrease, however not statistically significant, in both percent aggregation and number of aggregates per cell, as shown in Figure 19.

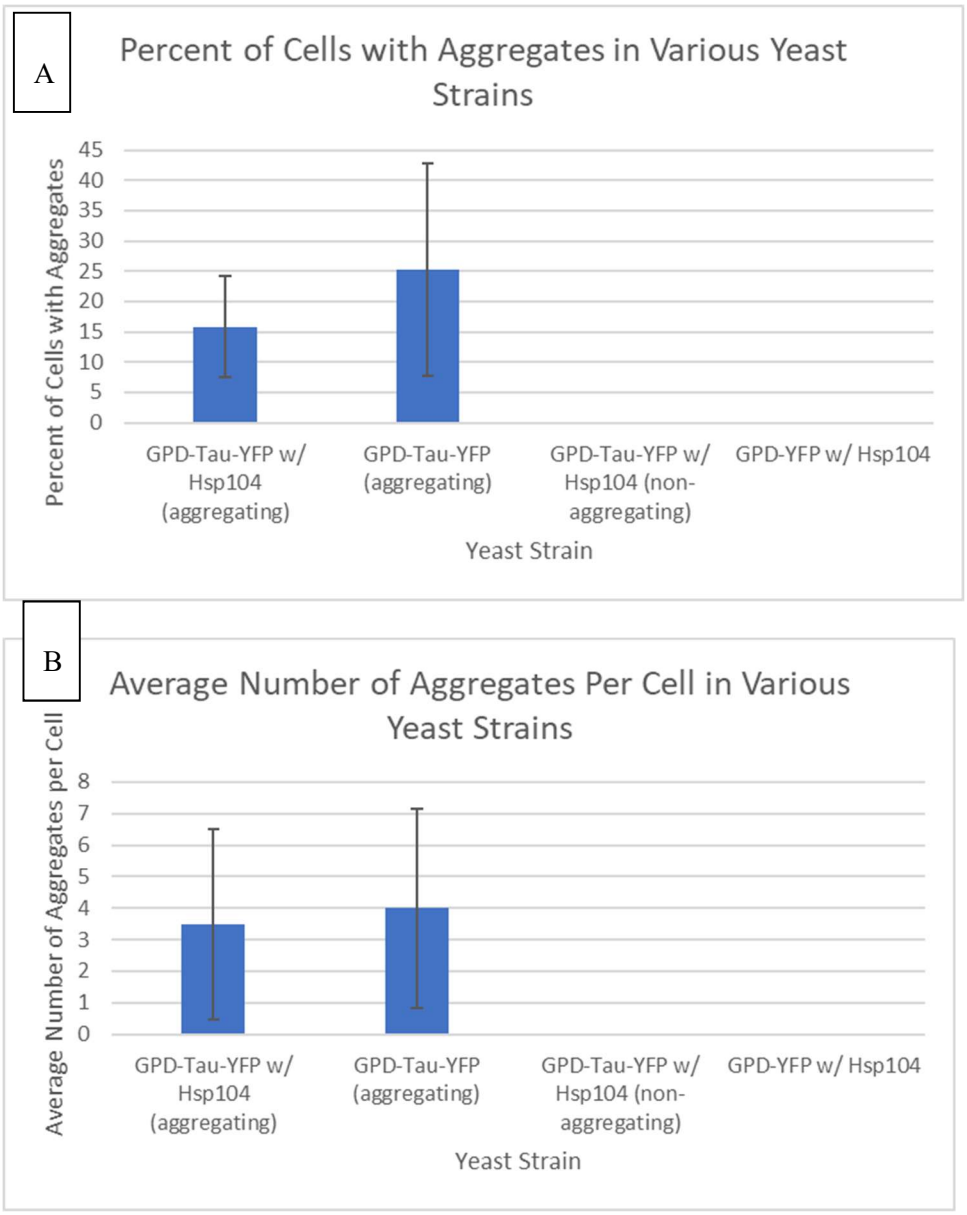

Figure 19. Effects of Hsp104 on tau aggregation. (A) Percent aggregation of tau in aggregating and non-aggregating strains, with and without Hsp104. Hsp104 does not

significantly decrease the percent of cells showing aggregation in either of the aggregating strains. (B) Average number of tau aggregates per yeast cell. Hsp104 does not significantly decrease the average number of tau aggregates per cell.

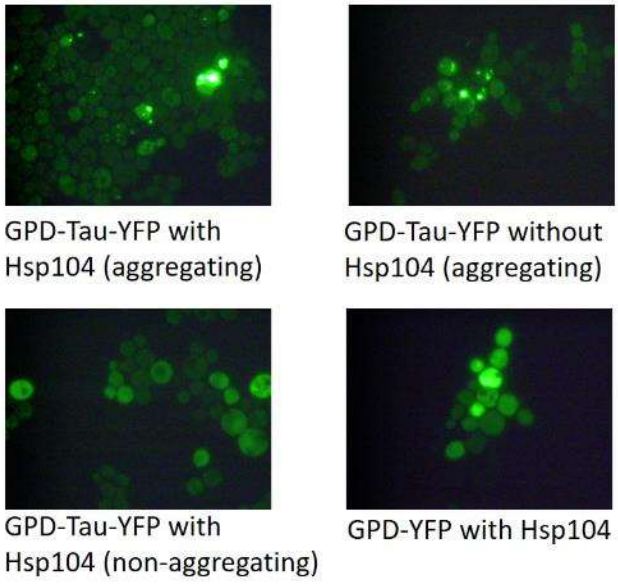

Figure 20. Aggregates of tau in various yeast strains. Tau aggregation is transformant-specific and occurs consistently in the same strains. No aggregates were seen in the designated non-aggregating strain or the empty control plasmid. Hsp104 did not significantly cure tau aggregates.

5.3 Discussion

Our results confirm that tau in yeast is an accurate model for various tauopathies. It behaves similarly in yeast as it does in humans, implying that its properties are inherent to the protein itself and not its cellular environment. The fact that it still aggregates in diploid strains may be important in further colocalization experiments or any tests involving yeast mating. Despite our expectations, Hsp104, a known yeast disaggregase, did not

significantly cure tau aggregates. On average, a slight dip in percentage aggregation was observed, but it was not significant enough to qualify as curing the tau aggregates. There are several potential explanations for this. Firstly, tau is not a native yeast protein, so it is possible that Hsp104, a yeast disaggregase, would not be able to cure a non-yeast protein. Alternatively, tau may form aggregates that are not sensitive to Hsp104; the usual targets of Hsp104 are rich in glutamine and asparagine, while tau is not. We also found that, despite the focus on insoluble aggregates of proteins involved in AD, even the aggregating strains of tau did not form detergent-insoluble aggregates, forming soluble monomers instead. This is interesting, as it would seem to corroborate the claims of Fox *et al.* that soluble species of tau, not neurofibrillary tangles, are the toxic species observed in AD that are responsible for the disruption of hippocampal function (21).

5.4 Conclusions

- MAPT repeat domain 244-372 can form fluorescent foci in yeast strains in the presence and absence of pre-existing prions; however, its aggregation is transformant-specific.
- Our data indicates that the wild-type repeat domain aggregates are not not detergent-insoluble.
- Over-expression of Hsp104 does not cure the strains containing tau aggregates.

5.5 Future Work

We have preliminary data to suggest that the aggregation of a pro-aggregation mutant of the repeat domain is capable of forming aggregates; however, this is not transformant specific. We will be testing the pro-aggregation strain of tau, as well as the full-length tau,

with SDD-AGE to determine if their aggregates are also detergent-insoluble. To determine if the aggregating strains of tau are in fact phosphorylated, we plan to run a Phos-tag gel on the aggregating and non-aggregating strains. Finally, we plan to test for colocalization with both Aβ and U1-70k to determine if aggregation between any two could be linked.

APPENDIX A. TABLES OF STRAINS, PRIMERS, PLASMIDS, AND DATA

Table A1: Strains used in this work

Name	Source	Genotype
GT81-C	Chernoff et al 2000	MAT a ade1-14 his3-Δ200 or 11,15 leu2-3,112 lys2 trp1 ura3-52 y+ PIN+
GT159	Chernoff et al 1999	a ade1-14 his3-Δ200 or 11,15 leu2-3,112 lys2 trp1-Δ ura3-52 Ψ-PIN + cl. 4
GT197	Chernoff et al 2000	a ade1-14 his3-Δ200 or 11,15 leu2-3,112 lys2 trp1-Δ ura3-52 Ψ-pin-?
GT409	Chernoff et al 2000	a ade1-14 his3-Δ200 or 11,15 leu2-3,112 lys2 trp1-Δ ura3-52 Ψ-pin-

Table A2: Plasmids used in this work

Plasmid name	Yeast marker	Collection number	Source
pCUP1-YFP	Leu2	1585	Chernoff Russian Lab
pGPD-YFP	*URA3*	1588	Chernoff Russian Lab
pGPD-Tau(244-372)-YFP	*URA3*	1592	Chernoff Russian Lab
pCup1-U1-70kNM-YFP	*Leu2*	1600	Chernoff Lab
pCup1-Abeta(1-42)-CFP	*URA3*	1607	Chernoff Lab
PCup1-U1-70kF-YFP	*Leu2*	1614	Chernoff Russian Lab
pCup-U1-70kN(1-99)-YFP	*Leu2*	1636	This work
pCup-U1-70kM(100-181)-YFP	*Leu2*		This work

Table A3: Primers used in this work

Primer name	Collection number	Use
U1-70kN BamHI For	1263	Forward primer for amplifying the N-terminal region of U1-70k, plus adding a BamHI restriction site
U1-70kN XbaI Rev	1264	Reverse primer for amplifying the N-terminal region of U1-70k, plus adding a XbaI restriction site
U1-70k RRM XbaI Reverse	1265	Reverse primer for amplifying the RRM region of U1-70k, plus adding a XbaI restriction site
U1-70kC BamHI For	1266	Forward primer for amplifying the C-terminal region of U1-70k, plus adding a BamHI restriction site
U1-70k Full Rev	1267	Reverse primer for amplifying the Full region of U1-70k, plus adding a XbaI restriction site
U1-70kM BamHI F	1308	Forward primer for amplifying U1-70KM (100-181) with BamHI cut site

REFERENCES

1. Aguzzi, A. and O'Connor, T. (2010). Protein aggregation diseases: pathogenicity and therapeutic perspectives. *Nature Reviews Drug Discovery*, 9, 237-248.
2. Alzheimer's Association (2017). Alzheimer's disease facts and figures. *Alzheimer's & Dementia: The Journal of the Alzheimer's Association*, 13(4), 325-373.
3. Bai B., Hales C.M., Chen P.C., Gozal Y., Dammer E.B., Fritz J.J., Wang X., Xia Q., Duong D.M., Street C. et al. (2013) U1 small nuclear ribonucleoprotein complex and RNA splicing alterations in Alzheimer's disease. *Proc. Natl Acad. Sci. U.S.A.*, 110 (41), 16562–16567
4. Berson, J.F., Theos, A.C., Harper, D.C., Tenza, D., Raposo, G., and Marks, M.S. (2003). Proprotein convertase cleavage liberates a fibrillogenic fragment of a resident glycoprotein to initiate melanosome biogenesis. *The Journal of Cell Biology*, 161(3), 521-533.
5. Diner I., Hales C.M., Bishof I., Rabenold L., Duong D.M., Yi H., Laur O., Gearing M., Troncoso J., Thambisetty M., Lah J.J., Levey A.I., and Seyfried N.T. (2014) Aggregation properties of the small nuclear ribonucleoprotein U1–70K in Alzheimer disease. *J Biol Chem*, 289(51), 35296–35313.
6. Hales, C.M., Dammer, E.B., Deng, Q., Duong, D.M., Gearing, M., Troncoso, J.C., and Seyfried, N.T. (2016). Changes in the detergent-insoluble brain proteome linked to amyloid and tau in Alzheimer's Disease progression. *Proteomics*, 16(23), 3042–3053.
7. Hales, C.M., Dammer, E.B., Diner, I., Yi, H., Seyfried, N.T., Gearing, M., Glass, J.D., Montine, T.J., Levey, A.I., and Lah, J.J. (2014). Aggregates of small nuclear ribonucleic acids (snRNAs) in Alzheimer's disease. *Brain Pathol.*, 24(4), 344-351.
8. Hernández, H., Makarova, O.V., Makarov, E.M., Morgner, N., Muto, Y., Krummel, D.P., and Robinson, C.V. (2009). Isoforms of U1-70k Control Subunit Dynamics in the Human Spliceosomal U1 snRNP. *PLoS One*, 4(9), e7202.
9. Knowles, T.P.J., Vendruscolo, M., and Dobson, C.M. (2014). "The amyloid state and its association with protein misfolding diseases". *Nature Reviews Molecular Cell Biology*, 15(6), 384–396.
10. Liebman, S.W. and Chernoff, Y.O. (2012). Prions in Yeast. *Genetics*, 191(4), 1041–1072.
11. Rocca, W.A., Petersen, R.C., Knopman, D.S., Hebert, L.E., Evans, D.A., Hall, K.S., and White, L.R. (2011). Trends in the incidence and prevalence of Alzheimer's disease, dementia, and cognitive impairment in the United States. *Alzheimer's & Dementia : The Journal of the Alzheimer's Association*, 7(1), 80–93.

12. Ross, C.A. and Poirier, M.A. (2004). Protein aggregation and neurodegenerative disease. *Nature Medicine*, 10 Suppl 1(7), S10-7.
13. Gietz, D., St Jean, A., Woods, R.A., and Schiestl, R.H. (1992). Improved method for high efficiency transformation of intact yeast cells. *Nucleic Acids Research*, 20(6), 1425-1426.
14. Bishof, I., Dammer, E., Duong, D., Kundinger, S., Gearing, M., Lah, J., Levey, A., and Seyfried, N. (2018). RNA-binding proteins with basic–acidic dipeptide (BAD) domains self-assemble and aggregate in Alzheimer's disease. *Journal of Biological Chemistry*, 293, 11047-11066.
15. Karran, E.H., Mercken, M.H., and Strooper, B.D. (2011). The amyloid cascade hypothesis for Alzheimer's disease: an appraisal for the development of therapeutics. *Nature Reviews Drug Discovery*, 10, 698-712.
16. Murphy, M.P. and LeVine, H. (2010). Alzheimer's disease and the amyloid-beta peptide. *Journal of Alzheimer's Disease*, 19(1), 311-23.
17. Mandelkow, E.M. and Mandelkow, E. (2012). Biochemistry and cell biology of tau protein in neurofibrillary degeneration. *Cold Spring Harbor Perspectives in Medicine*, 2(7), a006247.
18. Wolozin, B. (2014). Physiological protein aggregation run amuck: stress granules and the genesis of neurodegenerative disease. Discovery Medicine, 17(91), 47-52.
19. Lee, V.M.-Y., et al. (2001). Neurodegenerative tauopathies. *Annual Review of Neuroscience*, 24(1), 1121-1159.
20. Wood, J.G., Mirra, S.S., Pollock, N.J., and Binder, L.I. (1986). Neurofibrillary tangles of Alzheimer disease share antigenic determinants with the axonal microtubule-associated protein tau (tau). *Proc. Natl. Acad. Sci. U.S.A.*, 83, 4040–4043.
21. Fox, L.M., William, C.M., Adamowicz, D.H., Pitstick, R., Carlson, G.A., Spires-Jones, T.L., and Hyman, B.T. (2011). Soluble tau species, not neurofibrillary aggregates, disrupt neural system integration in a tau transgenic model. *Journal of neuropathology and experimental neurology*, 70(7), 588-595.
22. Epis, R., Marcello, E., Gardoni, F., and Di Luca, M. (2012). Alpha, beta-and gamma-secretases in Alzheimer's disease. *Front Biosci. (Schol. Ed.)*, 4, 1126-1150.